General Disclaimer

One or more of the Following Statements may affect this Document

ATS-6 MILLIMETER WAVELENGTH
PROPAGATION EXPERIMENT

D.B. Hodge, D.M. Theobold, and R.C. Taylor

The Ohio State University

ElectroScience Laboratory

Department of Electrical Engineering
Columbus, Ohio   43212

ITEM I FINAL REPORT
Report 3863-6

January 1976

NATIONAL AERONAUTICS & SPACE ADMINISTRATION
Goddard Space Flight Center
Greenbelt Road
Greenbelt, Maryland 20771

1. Report No.	2. Government Accession No.	3. Recipient's Catalog No.
4. Title and Subtitle ATS-6 MILLIMETER WAVELENGTH PROPAGATION EXPERIMENT		5. Report Date January 1976
		6. Performing Organization Code
7. Author(s) D.B. Hodge, D.M. Theobold, & R.C. Taylor		8. Performing Organization Report No. ESL 3863-6
9. Performing Organization Name and Address The Ohio State University ElectroScience Laboratory, Department of Electrical Engineering, Columbus, Ohio 43212		10. Work Unit No.
		11. Contract or Grant No. NAS5-21983
		13. Type of Report and Period Covered
12. Sponsoring Agency Name and Address NASA, GSFC Greenbelt, Maryland 20771 E. Hirschmann, Code 951, Technical Officer		Item I Final Report 14 Jan.'75-31 Jan.'76
		14. Sponsoring Agency Code 60

15. Supplementary Notes

16. Abstract

This report summarizes the OSU participation in the ATS-6 Millimeter Wavelength Propagation Experiment. Attenuation was measured simultaneously at 20 and 30 GHz on earth-space propagation paths to two ground terminals located at Columbus, Ohio. In addition, 20 and 30 GHz radiometric temperatures were measured along the same propagation paths; and the 20 GHz radiometric temperature was also measured at a third ground terminal.

The results of these measurements are presented, and diversity gains for the four pairs of propagation paths are discussed. The scintillation characteristics of the received signals are also presented.

17. Key Words (Selected by Author(s)) ATS-6 Scintillation Millimeter Wave Propagation Diversity		18. Distribution Statement	
19. Security Classif. (of this report) U	20. Security Classif. (of this page) U	21. No. of Pages 31	22. Price*

*For sale by the Clearinghouse for Federal Scientific and Technical Information, Springfield, Virginia 22151

CONTENTS

INTRODUCTION

The ATS-6 satellite was in a synchronous orbit located nominally at a longitude of 94° W for the majority of this experiment. This satellite had 20 and 30 GHz transmitters on board for the purpose of propagation measurements.

These signals were received by two OSU ground terminals (Fixed and Trans) located in Columbus, Ohio; both ground terminals were equipped with 20 and 30 GHz phase lock loop receivers as well as 20 and 30 GHz radiometers all sharing the same antenna aperture. A third OSU ground terminal (Unmanned) was instrumented with a 20 GHz radiometer only.

The ATS-6 satellite was on station and available for propagation measurements from 13 June 1974 to 19 May 1975. Both the 20 and 30 GHz signals were acquired by OSU on 13 June 1974. The nominal look angles for the OSU terminals during this period were an elevation of 40° and azimuth of 197°. Following this data period, the satellite was moved eastward to a station over India. Data were also gathered at the OSU terminals during this period until the satellite moved below the horizon on 13 June 1975.

The OSU Fixed and Transportable terminal antennas were located adjacent to each other initially at a spacing of 7 meters. Subsequently, the terminals were moved to the configuration shown in Fig. 1 for path diversity measurements. The triangular arrangement of the ground terminals was chosen to provide one baseline in the NW-SE quadrants to provide optimum diversity performance and for direct comparison with ATS-5 15 GHz diversity results. The second baseline was chosen to be E-W to permit comparison with Comsat 13 and 18 GHz uplink data.* And, finally, all three baselines were made nearly equal to allow direct comparison between the diversity pairs.

4.6 m Cassegrainian fed, parabolic antennas were utilized at both the Fixed and Unmanned receiver terminals; a 1.5 m focal point feed antenna was employed at the Unmanned radiometer terminal. The PLL receiver bandwidths ranged from 48 to 65 Hz. All data were digitized in real time at sample rates of either 1, 10, or 200 Hz, depending upon the mode of operation. The system margins on both the 20 and 30 GHz downlinks ranged from 35 to 55 dB during the course of the experiment. More detailed descriptions of the experiment and the associated hardware were presented in References 1, 2, 3, and 4. Initial results of this experiment as well as a development of an empirical relationship for diversity gain were presented in Reference 5.

---

*Data from the COMSAT 13 and 18 GHz uplink experiment has not yet been made available. If this data is received and the attenuation records for common fade periods are suitable for analysis, the diversity gain for a 13 and 18 GHz E-W baseline could be compared with the OSU 20 GHz results for the same baseline.
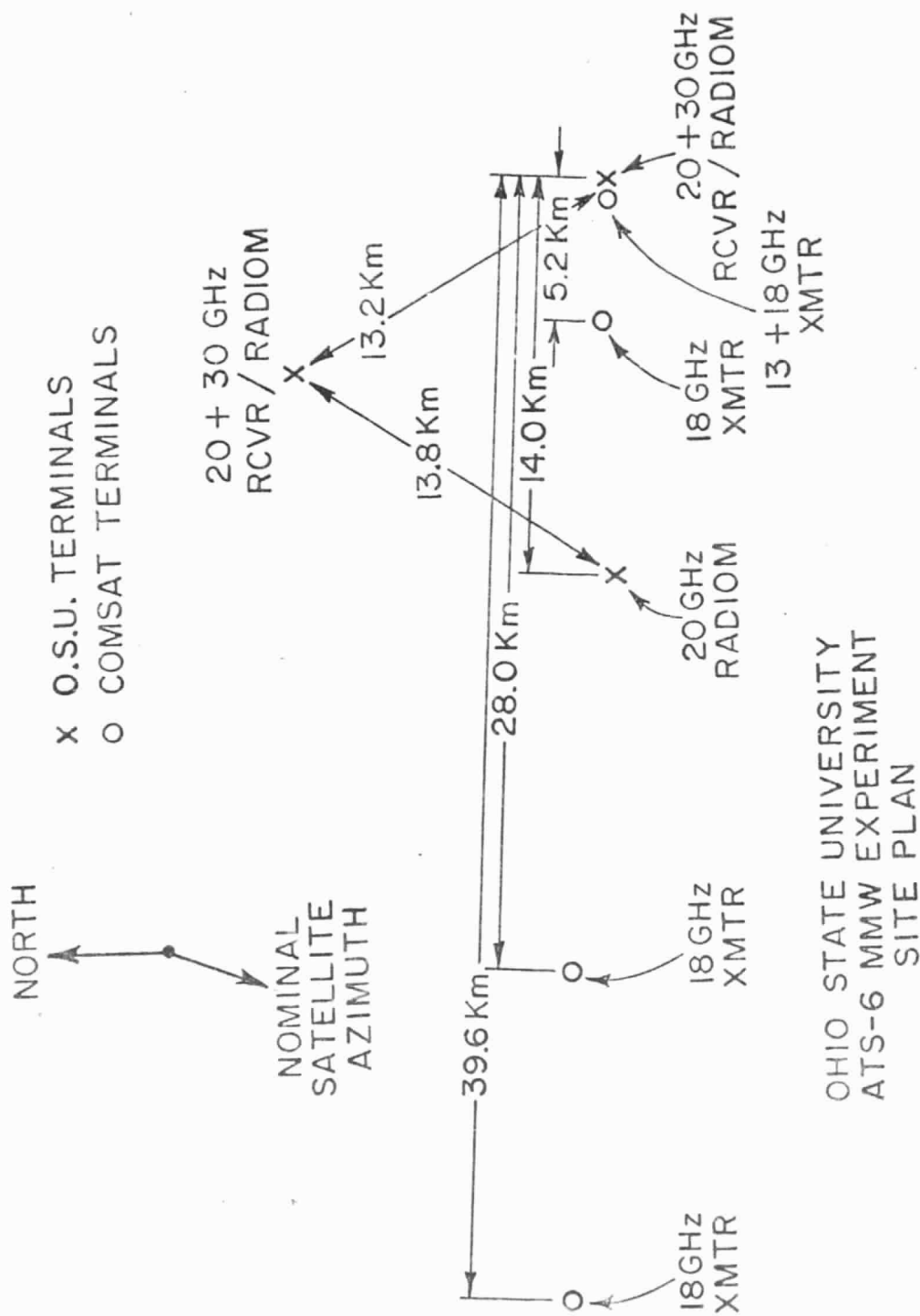
NORTH

x O.S.U. TERMINALS
o COMSAT TERMINALS

NOMINAL
SATELLITE
AZIMUTH

20 + 30 GHz
RCVR / RADIOM

20 + 30 GHz
RCVR / RADIOM

13.2 Km

5.2 Km

18 GHz
XMTR

13 + 18 GHz
XMTR

13.8 Km

14.0 Km

20 GHz
RADIOM

28.0 Km

18 GHz
XMTR

OHIO STATE UNIVERSITY
ATS-6 MMW EXPERIMENT
SITE PLAN

39.6 Km

18 GHz
XMTR

Fig. 1. OSU ATS-6 MMW Experiment Site Plan.

2

DIVERSITY GAIN

The data base for the diversity gain analysis was formed by editing the entire data set. Receiver data during periods of satellite movement, i.e., change of satellite orientation, during periods of equipment malfunction, and during extended clear weather periods, i.e., signal excursions less than 2 dB, were deleted. During these periods and whenever one or both of the beacons were not available, radiometric inferred attenuation data were utilized in lieu of directly measured attenuation. The radiometric inferred attenuation was calculated from

$$A = 10 \log_{10} \frac{T_m}{T_m - T_s} \quad [dB] \tag{1}$$

where T_s is the measured sky temperature and T_m is the mean absorption temperature. The mean absorption temperature was taken to be 273°K.

The edited data were analyzed by terminal pairs, i.e., diversity gain data were generated for all periods when edited data were available from both terminals. The resulting single terminal and diversity pair fade distributions are shown in Figs. 2-5 for the three 20 GHz terminal pairs and the 30 GHz terminal pair, respectively. The diversity gain data for these four cases are shown in Fig. 6 as a function of single terminal fade depth. These results are within 1-2 dB of the 15 GHz diversity results obtained by OSU using the ATS-5 satellite. This variation is within the experimental accuracy of the experiment and indicates that diversity gain is relatively independent of frequency. There is also a slight trend for the E-W and NE-SW 20 GHz diversity gain results to fall below those for the NW-SE 20 GHz case. This behavior seems to indicate that diversity gain is also not strongly dependent on baseline orientation for baselines large enough to approach the optimum diversity performance case. It is likely that anisotropic rain cells would influence diversity gain to a greater degree for smaller separation distances.

Also shown in Fig. 6 is the empirical curve for diversity gain developed from OSU and BTL 15 GHz data (Ref. 5). This relationship is

$$G = a (1 - e^{-bD}) \tag{2}$$

where

$$a = A - 3.6 (1 - e^{-0.24A}) \tag{3}$$

$$b = 0.461 (1 - e^{-0.26A}) \tag{4}$$

and G is the diversity gain in dB, D is the terminal separation in km, and A is the single terminal fade depth in dB.
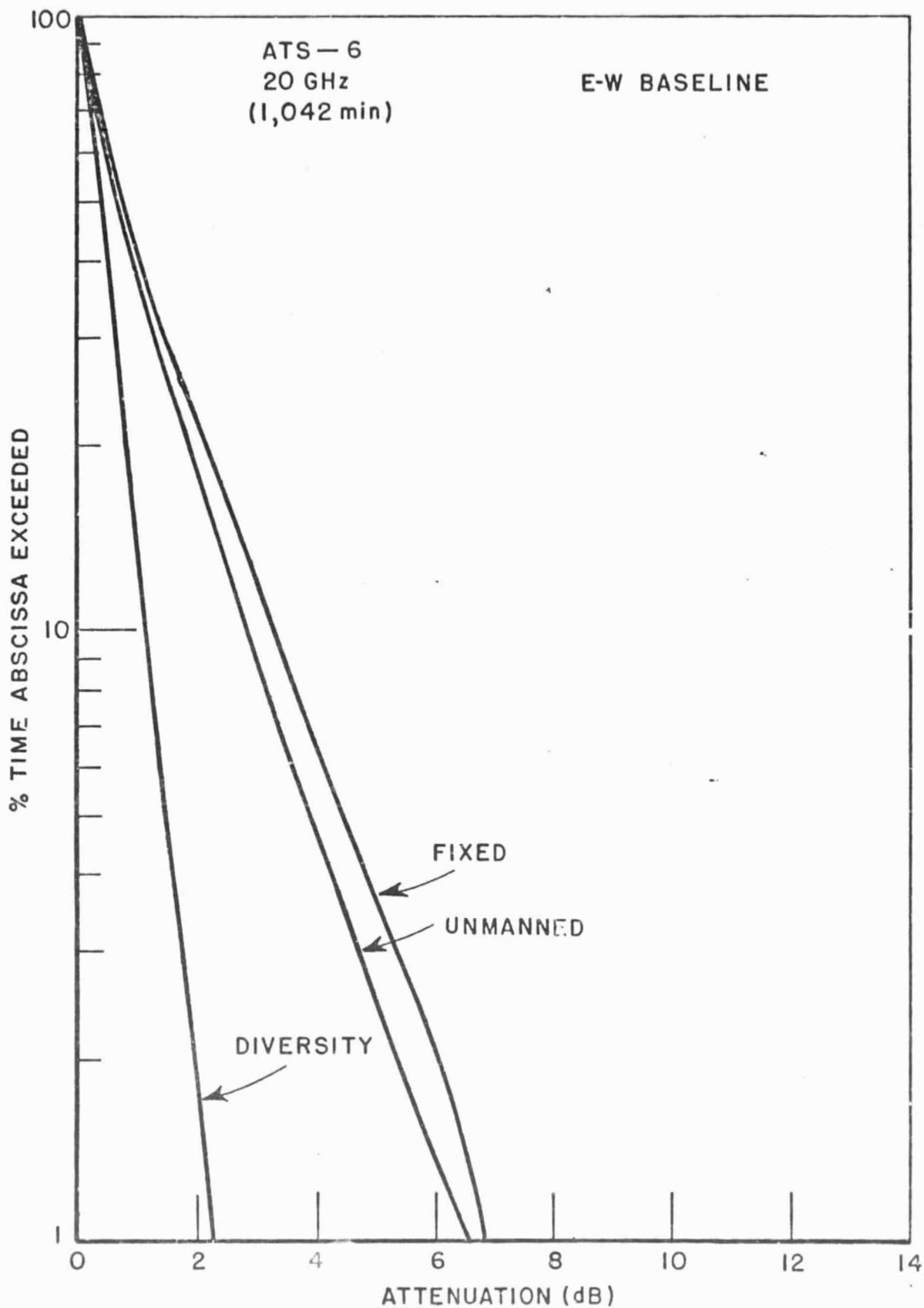
3

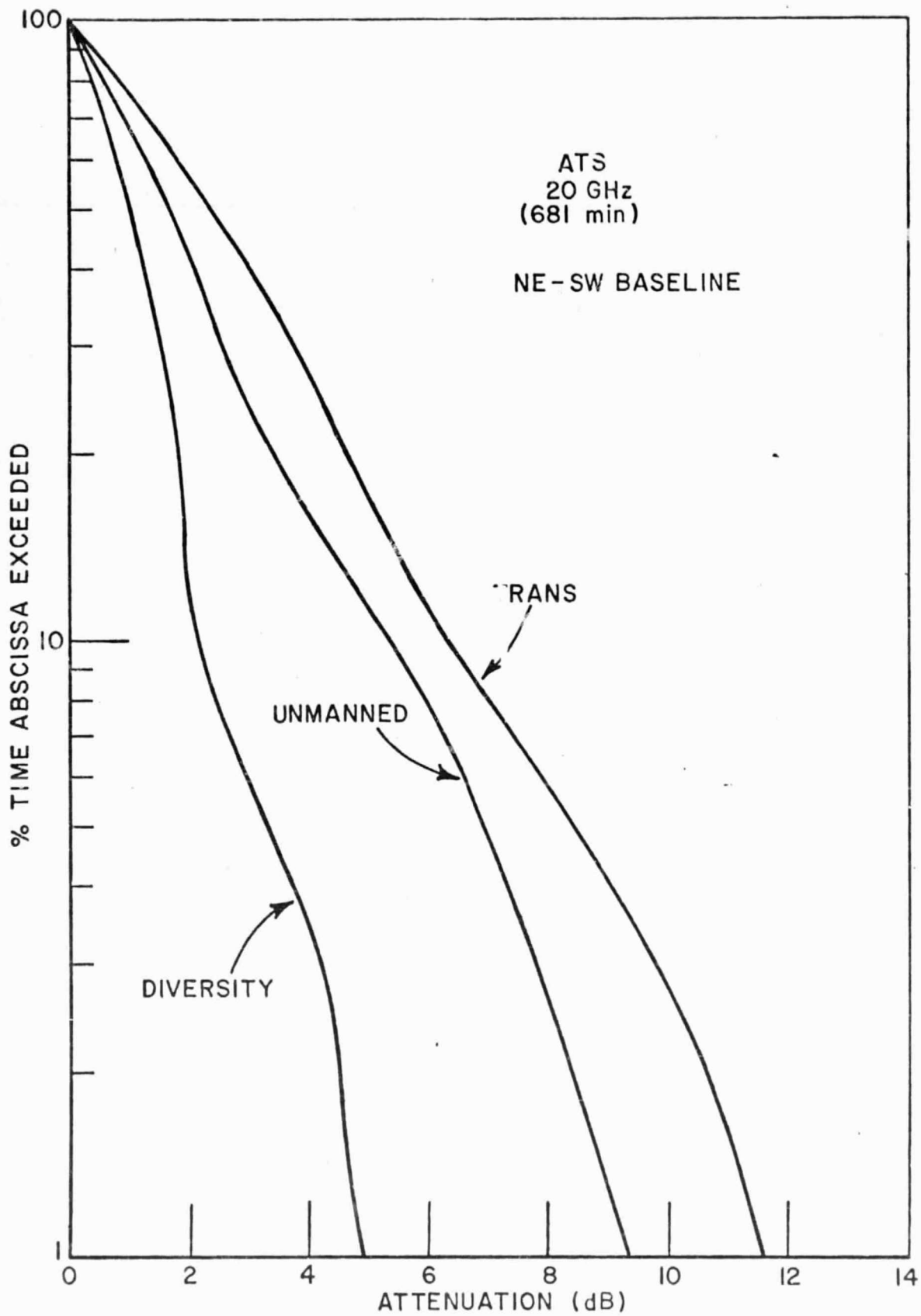Fig. 2.   20 GHz fade distributions, E-W baseline.

4

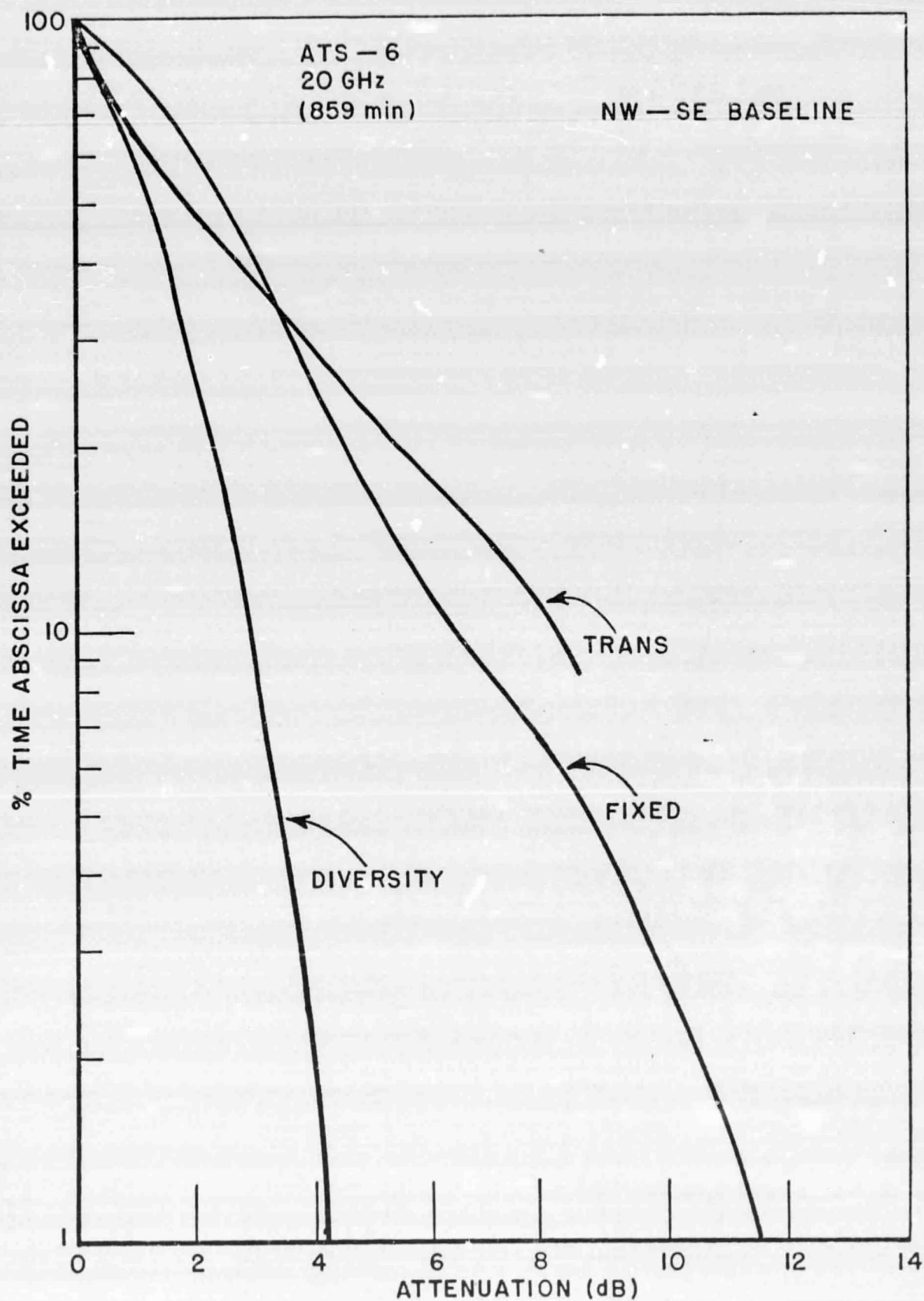Fig. 3. 20 GHz fade distributions, NE-SW baseline.

Fig. 4. 20 GHz fade distributions, NW-SE baseline.
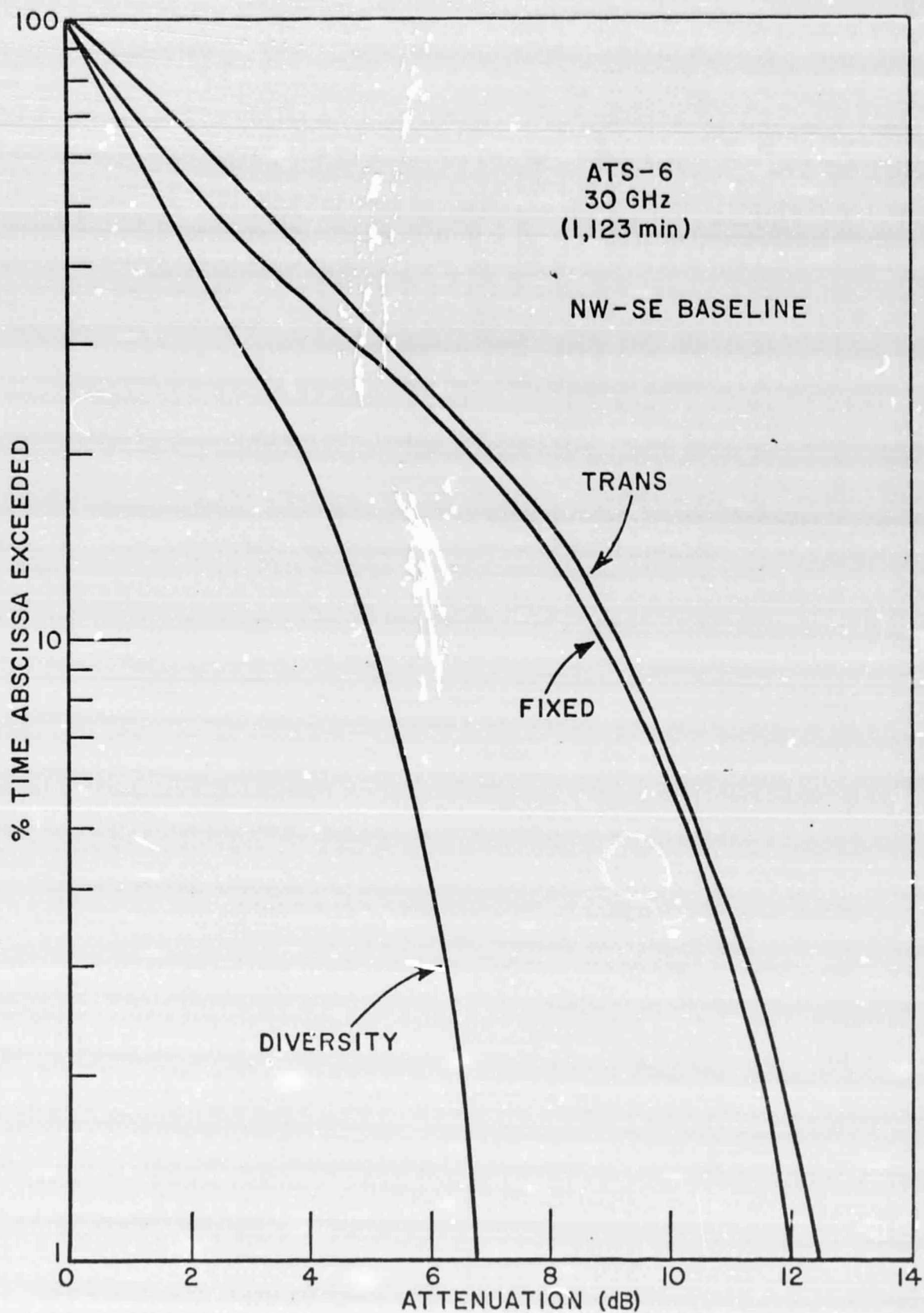
6

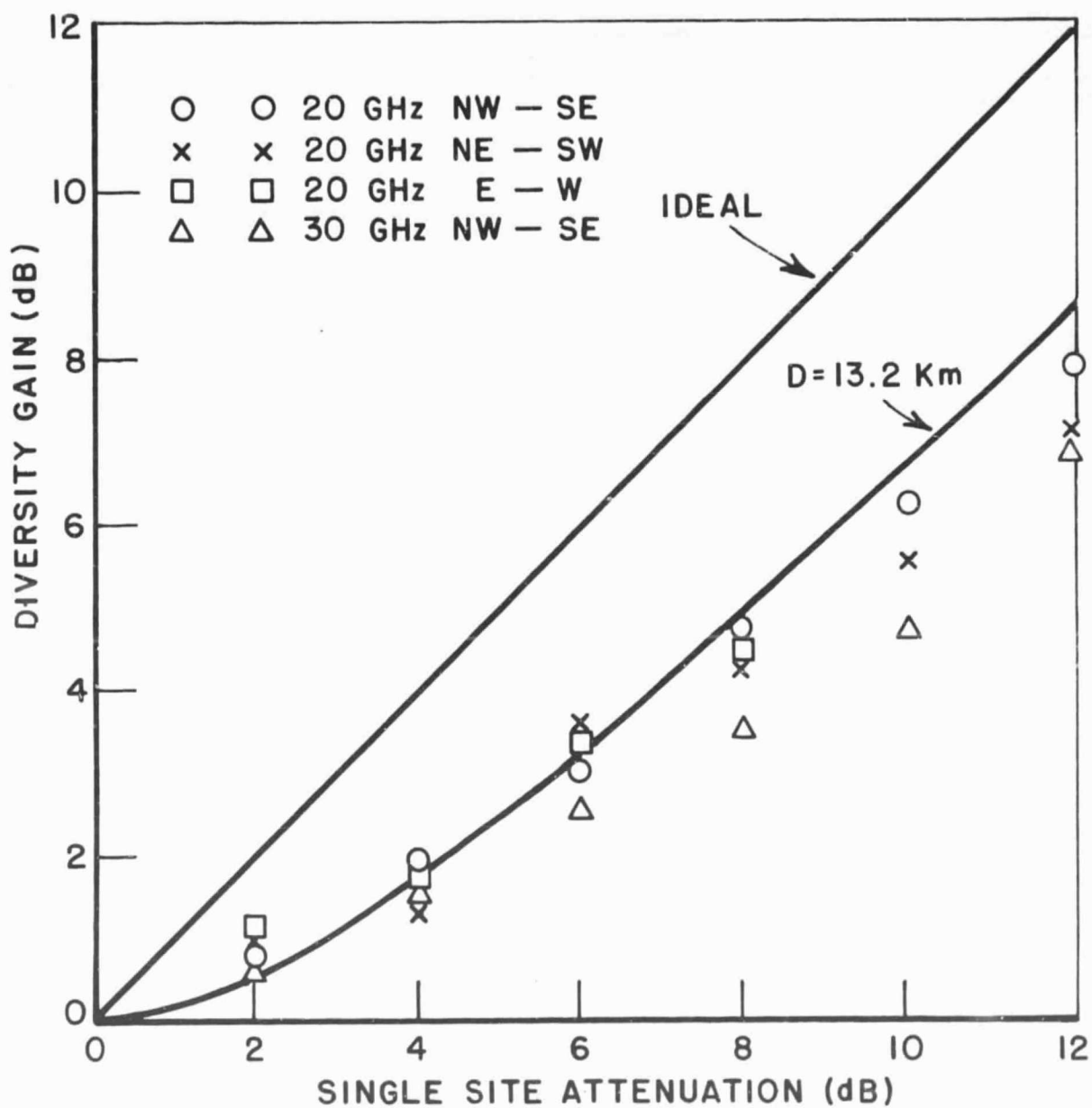Fig. 5. 30 GHz fade distributions, NW-SE baseline.

7

Fig. 6. Diversity gain vs. single site attenuation.

These data for the NW-SE baseline are replotted in Fig. 7 as functions of terminal separation distance along with the data used to generate the empirical relationship referred to above. Note that the 20 GHz data agrees quite well with the empirical relationship. Although the 30 GHz diversity gain tends to fall somewhat below the 15 and 20 GHz results for deeper fades, the disagreement is no greater than 1.5 dB.

SCINTILLATIONS

Rapid fluctuations of the 20 and 30 GHz signals received from the ATS-6 satellite were observed at OSU. These scintillations have been observed in clear air on a long term basis as well as on an event basis and also during precipitation fades. The peak-to-peak values, variance, power spectral density, and cross-correlation of these amplitude variations will be discussed in the following.

The data used in this discussion are voltage amplitudes which are directly proportional to the magnitude of the electric field incident upon the antenna at a given time t_i:

$$v(t_i) = C | E(t_i) | \tag{5}$$

where C is a constant and $||$ indicates magnitude. For a given number of data samples, N, the voltage amplitude is expressed in decibels by:

$$V(t_i) = 10 \log_{10} \frac{v(t_i)}{v_{max}} \quad ,$$

where v_{max} = maximum of $v(t_i)$, i = 1,2,...N.

Peak-to-Peak Amplitude Variations

Two categories of scintillation data may be established:

(i) those with small peak-to-peak variations which occur in clear air when observing the satellite at a high, e.g., 42°, elevation angle, and

(ii) those with larger amplitude excursions which occur during fade or cloud events or in a clear air at medium (20°) to low (2°) elevation angles.
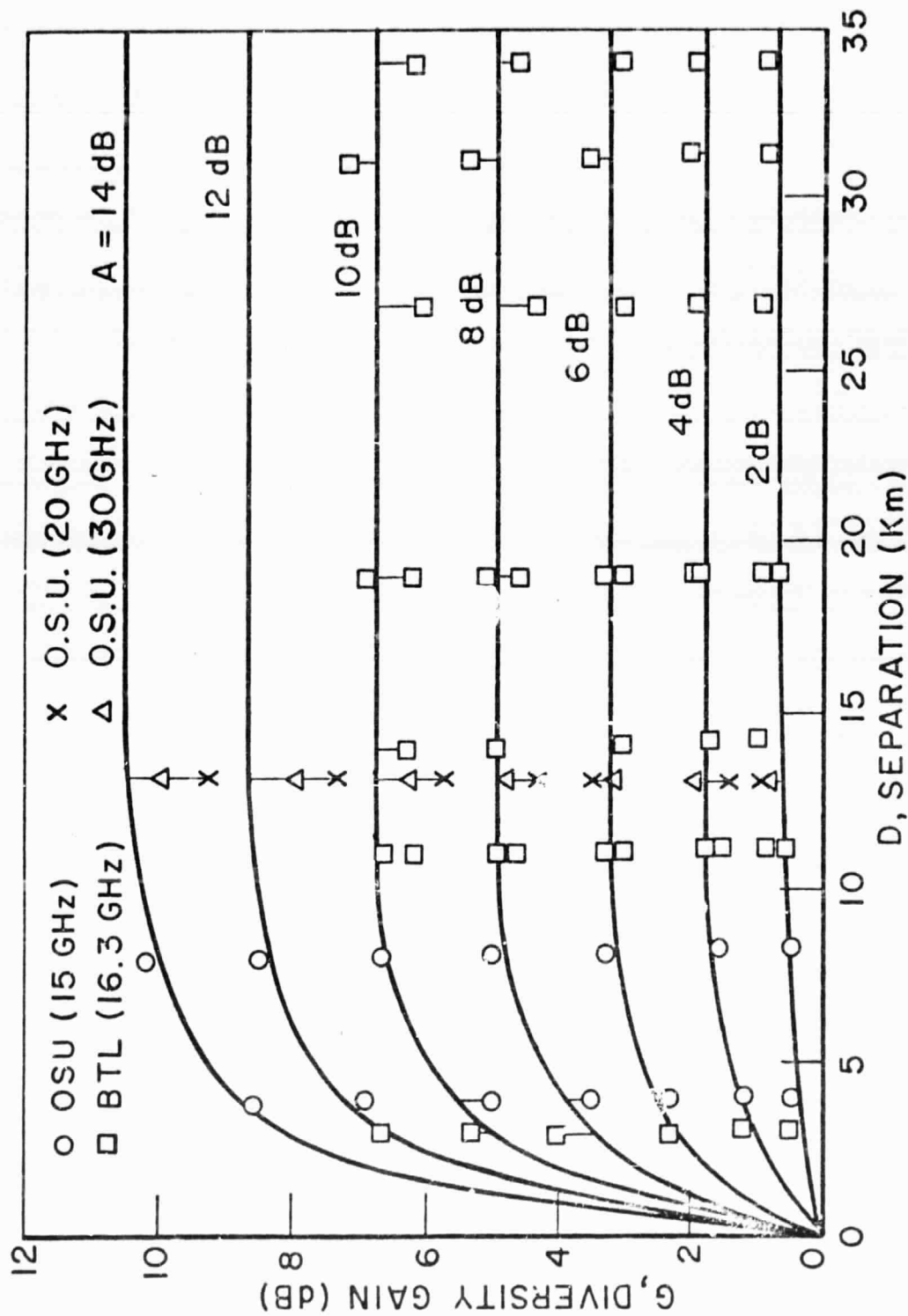
9

Fig. 7. Diversity gain vs. separation distance.

10

Figure 8 is a typical record of the 20 and 30 GHz signals when the satellite was located at a 42° elevation angle on a clear day. The amplitude excursions are less the 0.8 dB. These noise characteristics are typical for the clear air signal from the satellite over long periods of time.

Relatively short scintillation events on the order of 5 to 10 minutes duration have been observed in clear air at high elevation angles. Figure 9 is a record of such an event demonstrating excursions of 3 dB for about 8 minutes and then resuming a clear air character similar to that of Fig. 8. At a medium elevation angle (12°) a similar phenomenon was observed. Figure 10 shows an event superimposed upon a small fade and lasting about 7 minutes. Note that peak-to-peak variations during the fade are now 5 and 8 dB at 20 and 30 GHz, respectively, and the clear air excursions have increased to 1.5 and 2.5 dB at 20 and 30 GHz. This particular event began as a cloud was observed passing into the approximate path of the beam. At a low elevation angle of 2° in clear air, the amplitude excursions increase dramatically. Figure 11 shows variations of 20 and 30 dB at 20 and 30 GHz, respectively, which are characteristic of clear air observations made at low elevation angles.

These peak-to-peak amplitude variations suggest that several characteristics be examined. The amplitude scintillation depends on elevation angle, it is a function of time during short (5 to 10 minutes) events in clear air, and it is a function of time during precipitation fade events. These three topics are now examined by means of amplitude variance.

Amplitude Variance

The signal amplitude variance is expressed in decibels by:

$$\sigma^2 = 10 \log_{10} \frac{\sum_{i=1}^{N} [v(t_i) - \overline{v}]^2}{N \, \overline{v}^2} \tag{6}$$

where

$$\overline{v} = \frac{\sum_{i=1}^{N} v(t_i)}{N} \, . \tag{7}$$

Unless otherwise noted, the $v(t_i)$ are sampled at a rate of 200 samples/second and σ^2 is determined for $N = 2047$, i.e., a time interval of about 10 sec.

The variances for 20 and 30 GHz data were calculated from clear air data for elevation angles between 2° and 43° and are plotted in Fig. 12. The distribution of data suggested a cosecant behavior and, therefore, a minimum-mean-square error curve fit to $A \cdot [csc(\theta)]^B$ was made for the two data sets. The powers of $csc\theta$ were found to be
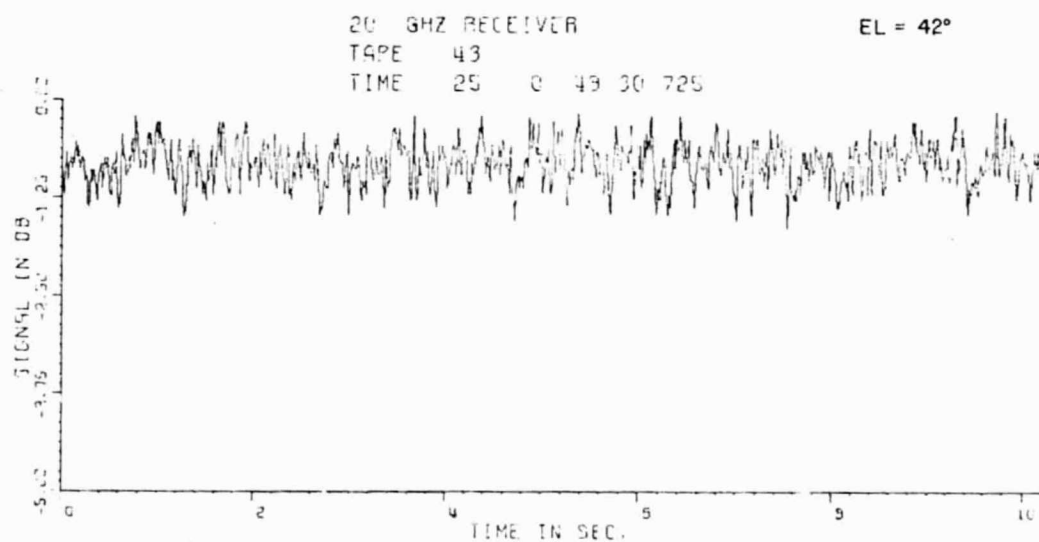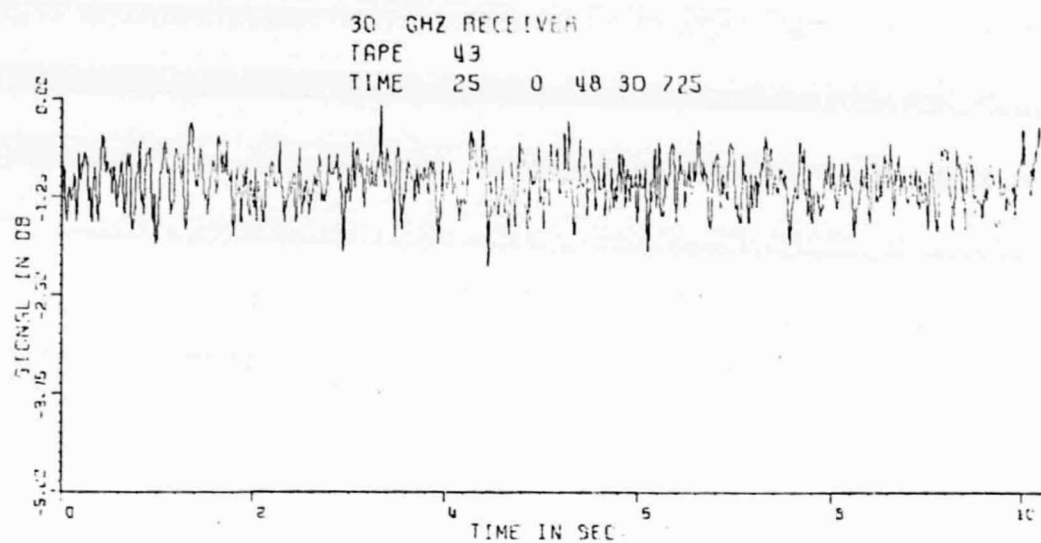
11

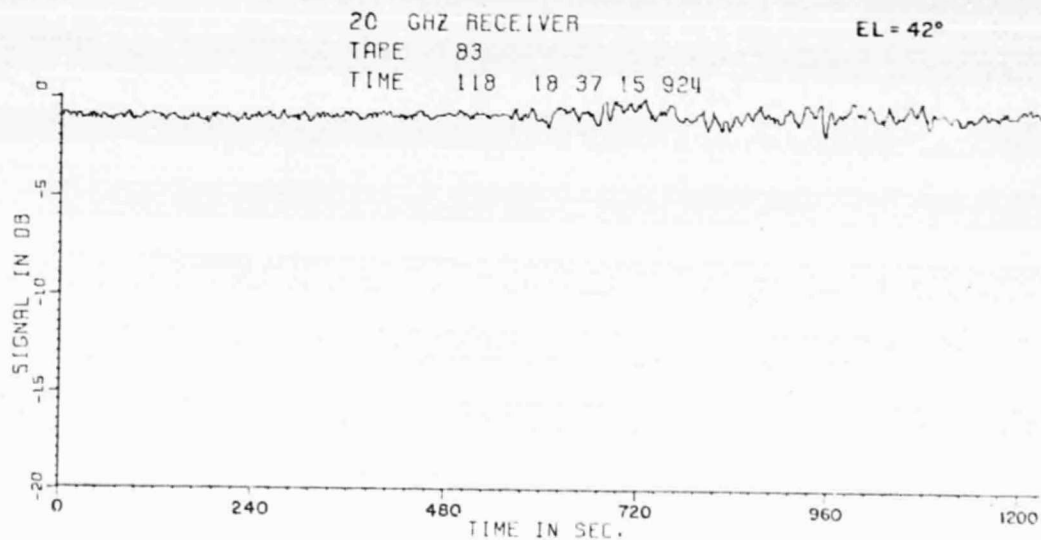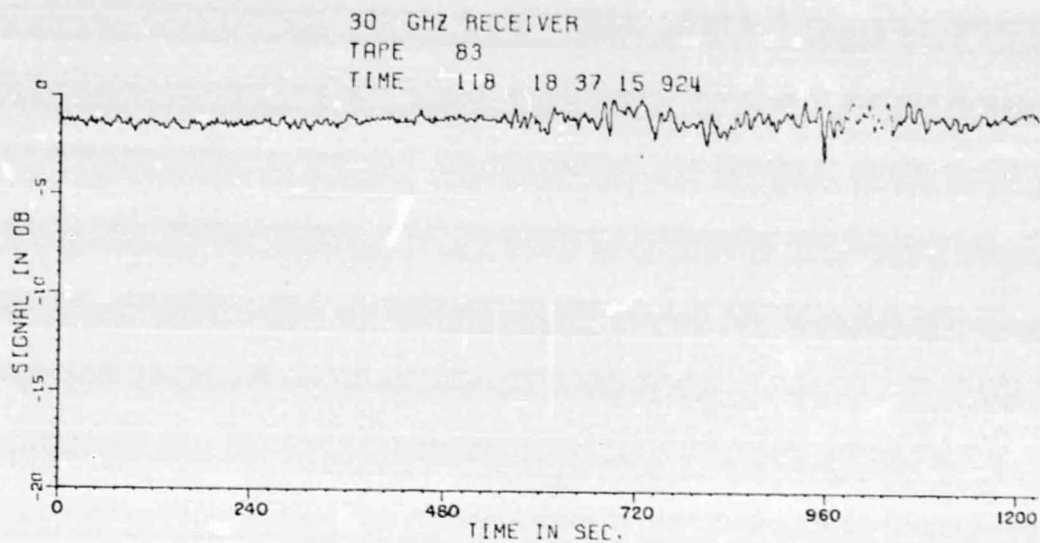Fig. 8. 20 and 30 GHz signal record at 42° elevation.

12

Fig. 9. Scintillation event at 42° elevation.

13

30 GHZ RECEIVER
TAPE 110
TIME 157 23 5 7 877

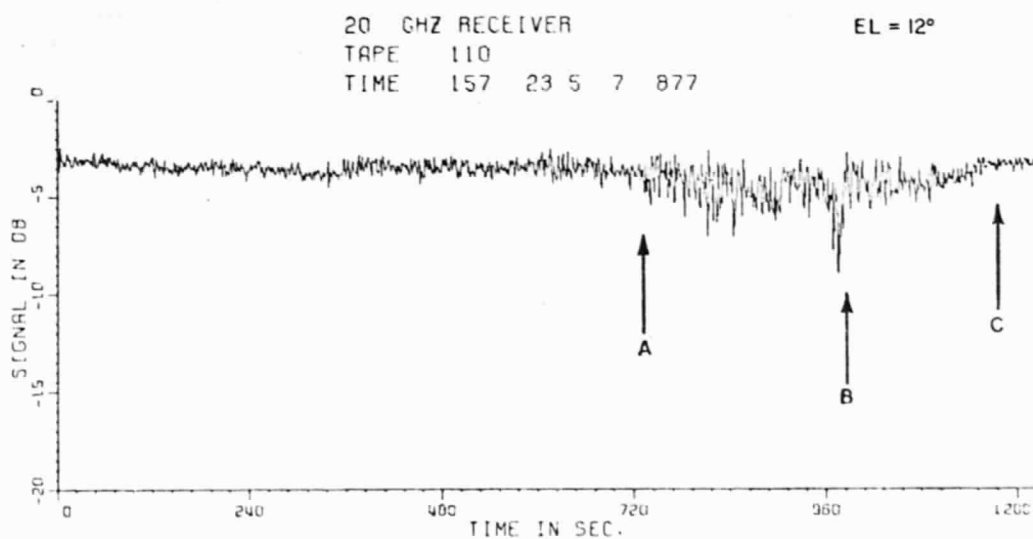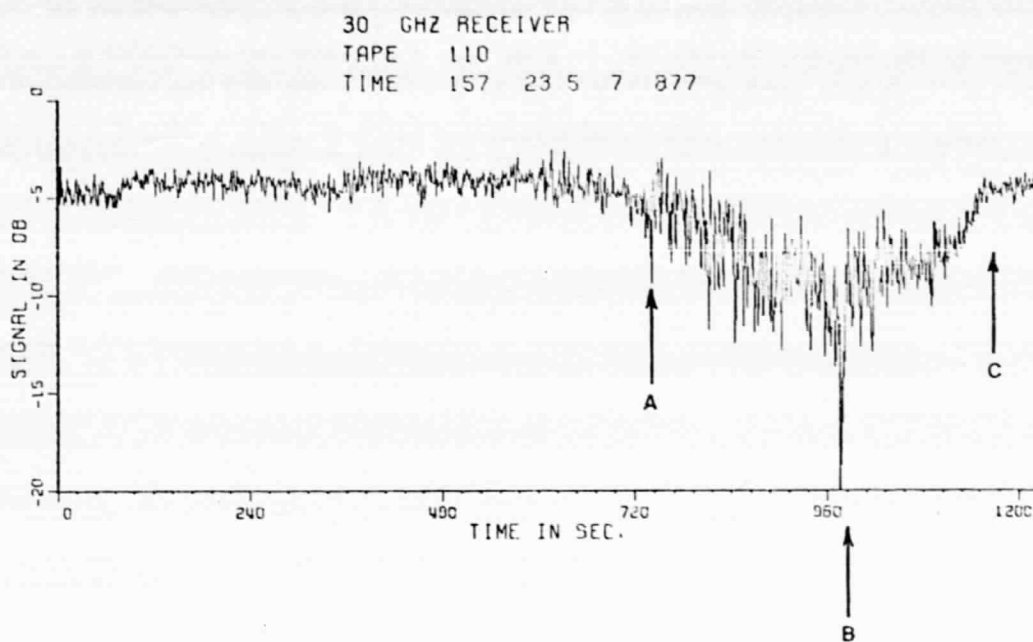20 GHZ RECEIVER   EL = 12°
TAPE 110
TIME 157 23 5 7 877

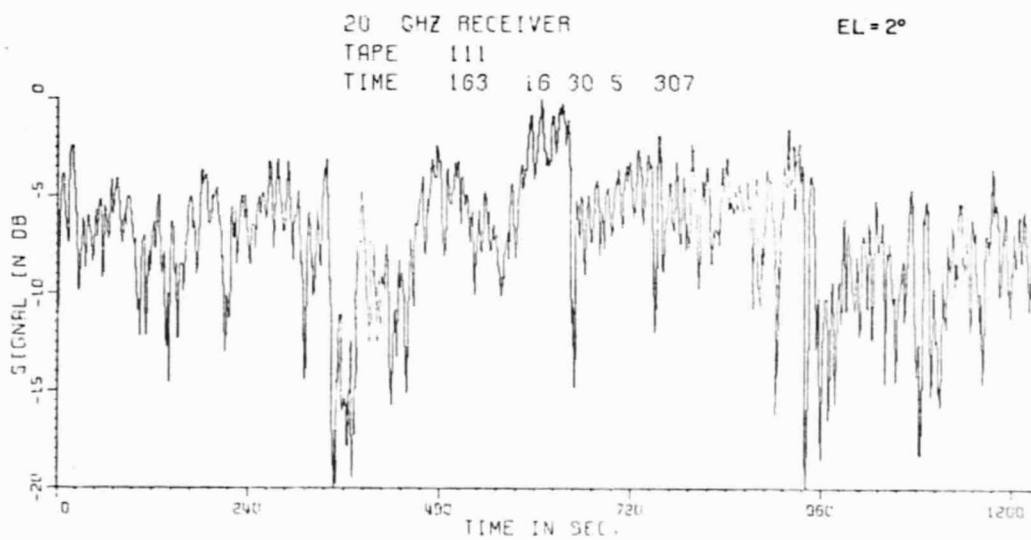Fig. 10. Fade and scintillation at 12° elevation.
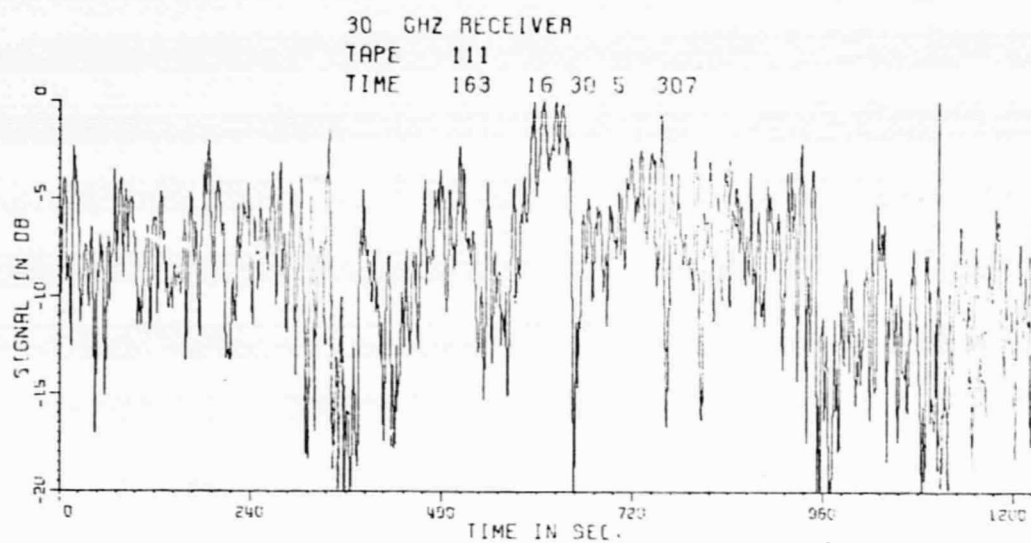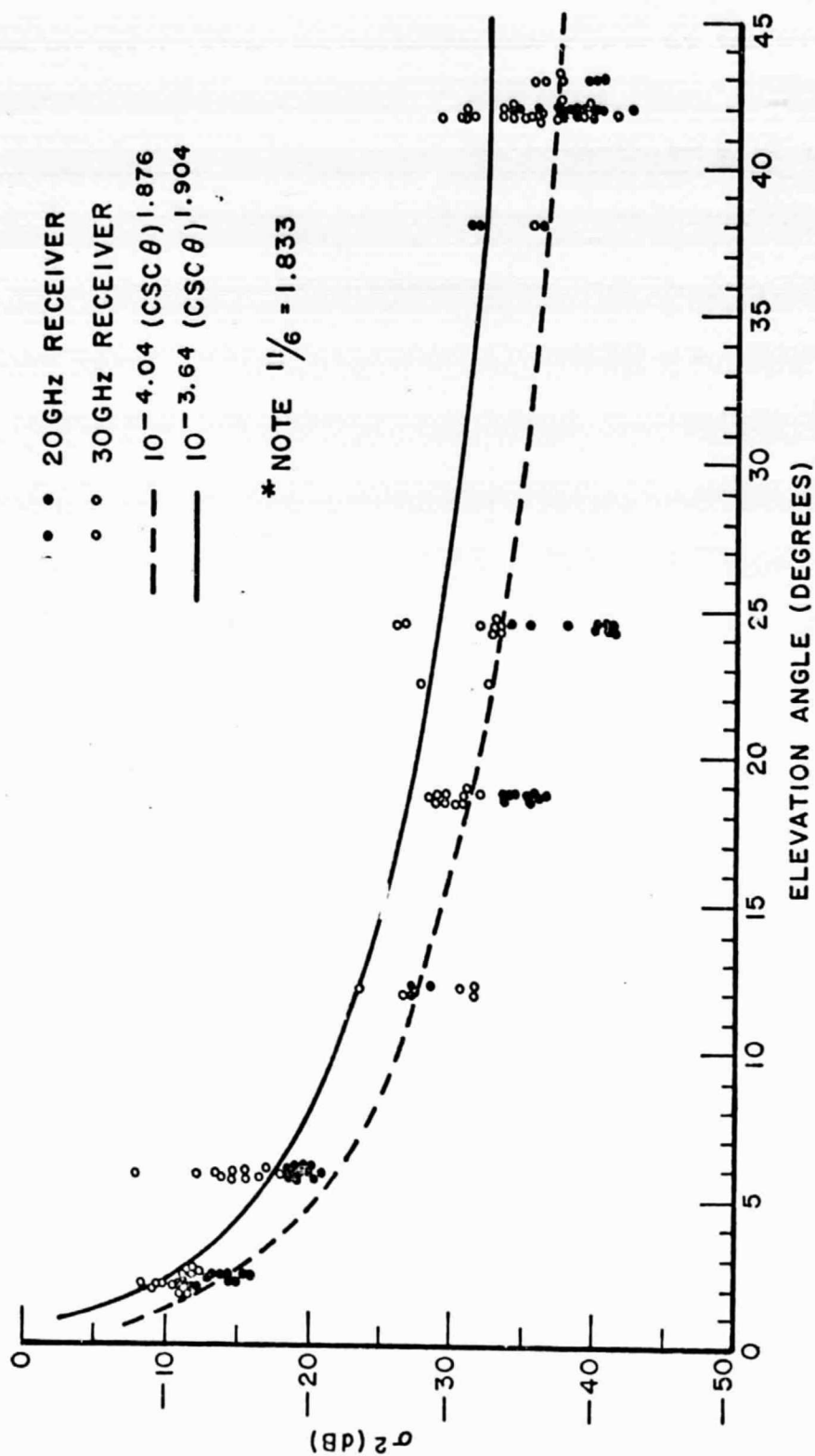
14

Fig. 11. Signal record at 2° elevation.

Fig. 12. Variance vs. elevation angle.

16

1.876 and 1.904 for 20 and 30 GHz, respectively. If $\csc\theta$ is regarded as directly proportional to the path length through the atmosphere, ℓ, and one notes that $11/6 = 1.833$, the data suggests that the amplitude variance follows a $\ell^{11/6}$ behavior. Thus, the variance of the amplitude scintillations observed appears to agree with that predicted for a Kolmogorov turbulence spectrum. A plot of the ratio $\sigma_{30}^2/\sigma_{20}^2$ versus elevation angle is shown in Fig. 13. The ratio is approximately constant, between 3 and 5 dB over a 30 dB range of variance, which suggests that this ratio is independent of path length.

Referring to Fig. 10, variance was calculated as a function of time during a scintillation event. The results are plotted in Fig. 14 for 20 and 30 GHz, and the arrows (A,B,C) correspond to those on Fig. 10. An increase in the variance of about 12 and 15 dB at 20 and 30 GHz, repectively, was observed during the event, followed by the expected clear air values. The points A, B, C on the two figures correspond to the onset, maximum, and end of the scintillation event.

Variance as a function of time was also calculated for the precipitation fade of about 4 minutes duration shown in Fig. 15. The variances for 20 and 30 GHz from both the Fixed and Transportable terminals are plotted in Fig. 16. The two terminals have a baseline separation of 7 meters in this example and the elevation angle was 43°. With arrows A, B, C corresponding to the onset, maximum, and end of the fade, note that the variance peaks prior to the event but does not reach a minimum until almost the end of the amplitude fade. One may speculate that a higher wind velocity or larger drop size distribution at the leading edge of a storm could account for such behavior. More data of this nature should be examined to determine whether or not this time lag between the amplitude fade depth and variance is a common characteristic of precipitation fade events.

The variance describes the RMS characteristics of amplitude variation as a function of path length and as a function of time during scintillation and fade events. More detailed frequency spectrum information will now be presented.

Power Spectral Density

The scintillation data from ATS-6 was also examined from the standpoint of power spectral density. If $V(f)$ is the Fourier transform of $v(t)$, then the power spectral density is defined as,

$$S(f) = |V(f)|^2 \qquad , \tag{8}$$

where f is the frequency in Hertz. All plots in this section are of magnitudes of $S(f)$ expressed in decibels below the mean carrier power unless otherwise noted.
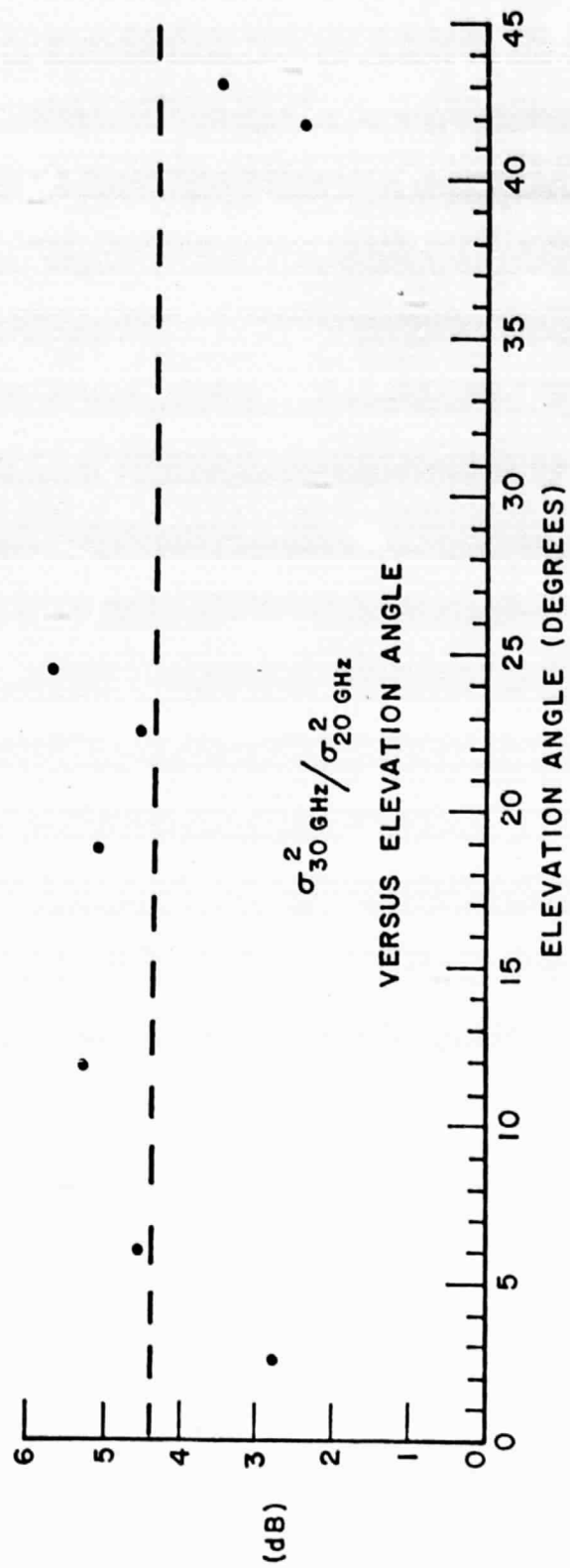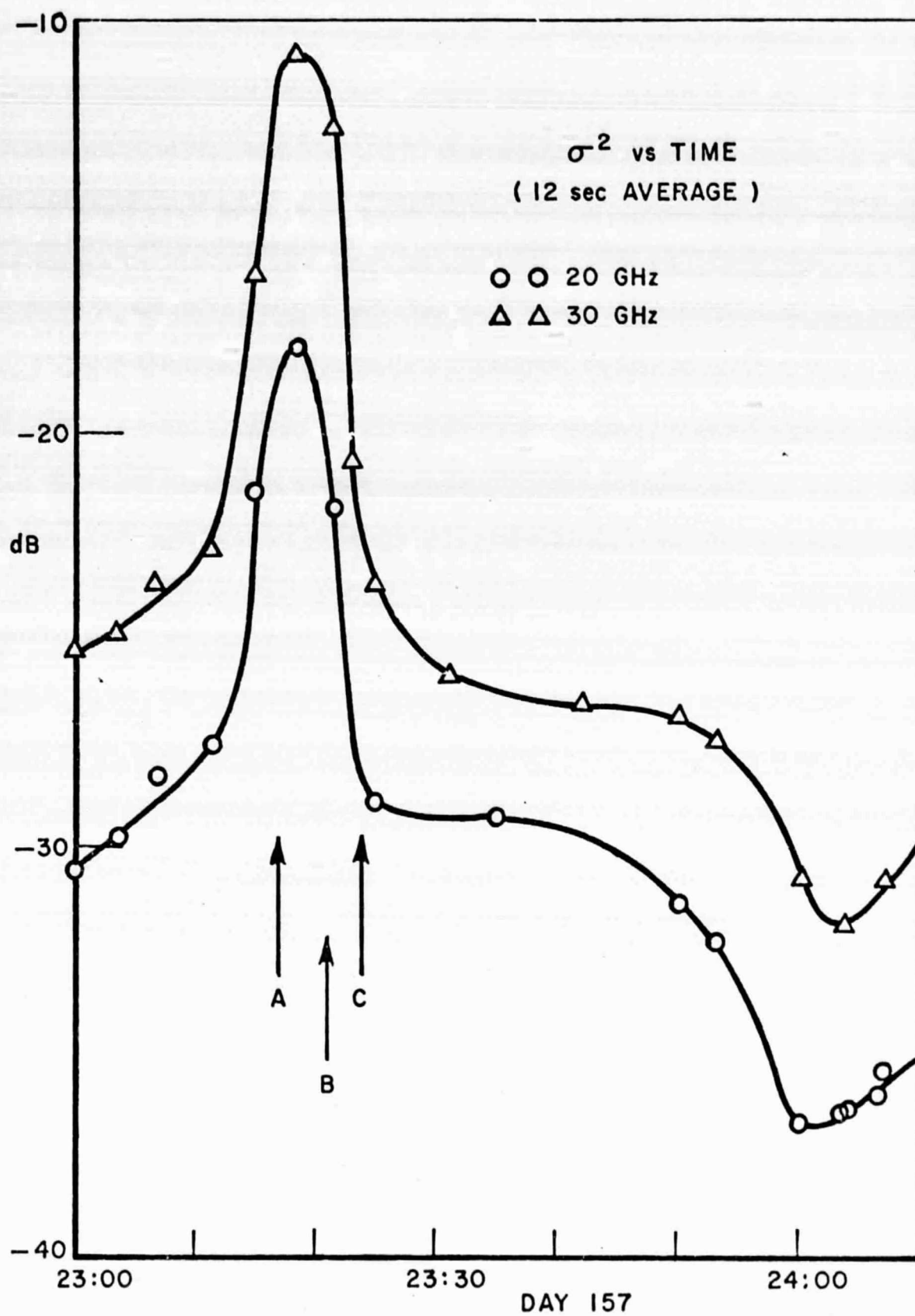
Fig. 13. Ratio of variances vs. elevation angle.
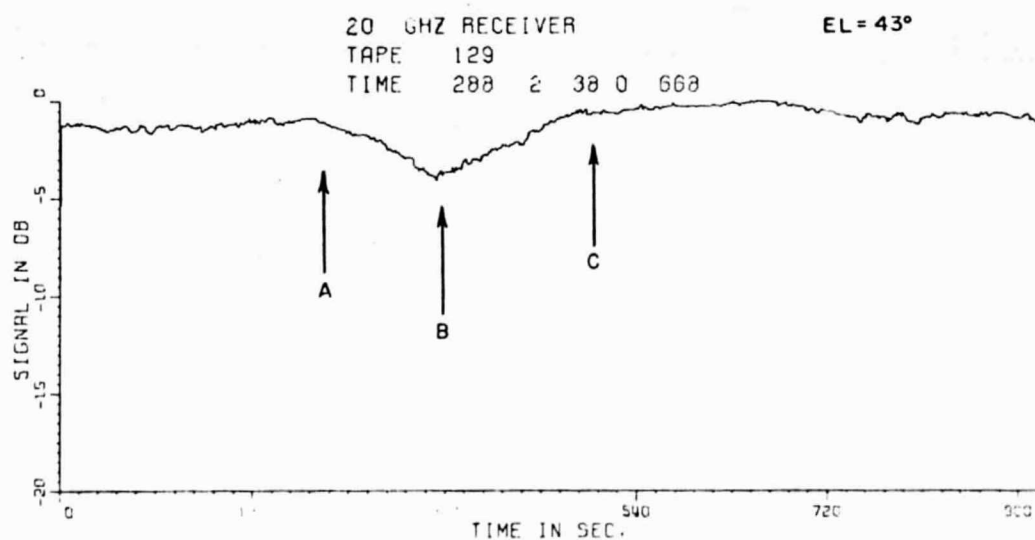
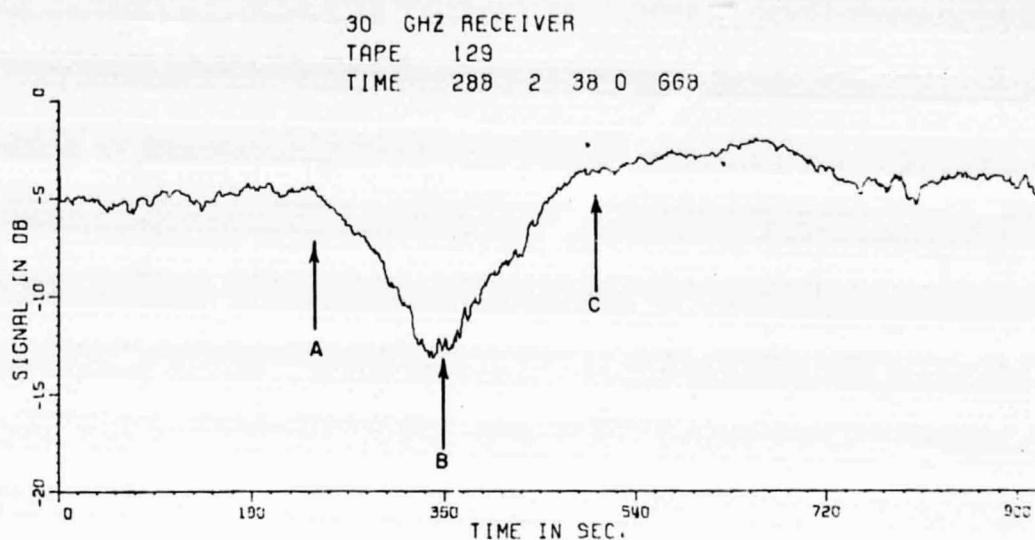Fig. 14. Variance vs. time (see Fig. 10).

19

Fig. 15. Fade event.

20

Fig. 16. Variance vs. time (see Fig. 15).

21

Figure 17 shows an example of the power spectrum in clear air at a high (42°) elevation angle. Note that the spectrum is relatively flat and the components above 2 Hz are very small. A clear air example at an elevation angle of 12° is examined in Fig. 18. This is a plot of the 30 GHz spectrum presented on a percent power basis over 0.05 Hz intervals. The behavior is very similar to that of Fig. 17.

The 30 GHz power spectrum of the scintillation event of Fig. 10 is shown in Fig. 18 below the clear air case. The scintillation causes a characteristic shift of energy downward in frequency. The sample interval for the spectrum calculation is only 10 sec.; therefore, it is unlikely that this shift is due to the lack of stationarity during the fade. Figure 19 shows the spectrum of a low elevation angle (2°) example. Here, the magnitude of the variations is much larger and the downward frequency shift of energy is also apparent.

The power spectrum may also be used to determine the correlation characteristics which are presented in the next section.

Cross-Correlation

The cross-correlation, $\rho_{12}(\tau)$, of two signals whose Fourier transforms are $V_1(f)$ and $V_2(f)$ may be determined from the inverse transform,
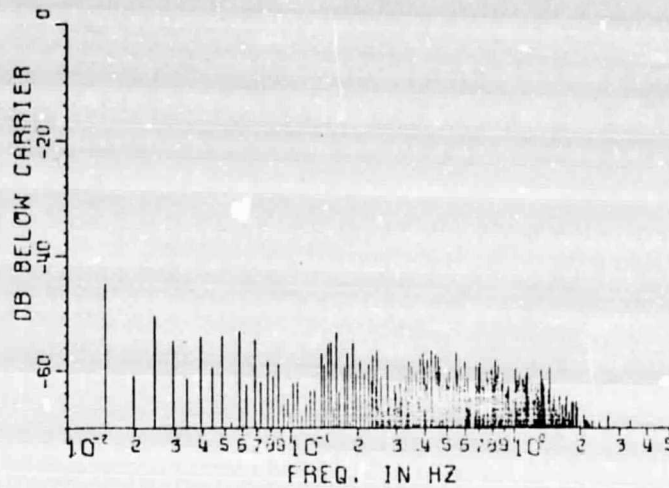
$$\rho_{12}(\tau) \longleftrightarrow V_1(f) \, V_2^*(f) \quad , \tag{9}$$

where ($\longleftrightarrow$) indicates a Fourier transform pair, τ is the time lag in seconds, and (*) denotes the complex conjugate. The following cross-correlation data are in terms of a correlation coefficient derived by this method.

20 and 30 GHz terrestrial beacon test signals were found to have a zero-lag correlation coefficient less than 0.1. However, the clear air data from the received satellite signal, presented in Fig. 20, have a correlation coefficient in excess of 0.8. Correlation coefficients of the range 0.8 to 0.9 were found to be representative of clear air data at all elevation angles. Hence, any phenomenon contributing to the 20-30 GHz correlation arises along the propagation path and not at the receivers. The example in Fig. 21 shows a zero-lag correlation coefficient of 0.9 for low elevation angle (2°). In general, correlation coefficients were found to be higher during scintillation and precipitation events than those calculated for clear air data.

The mechanism which causes the observed amplitude scintillations might be regarded as being either refractive or multipath in nature.

POWER SPECTRUM
30 GHZ RECEIVER
TAPE 110
TIME 142 17 10 13 905

POWER SPECTRUM   EL = 42°
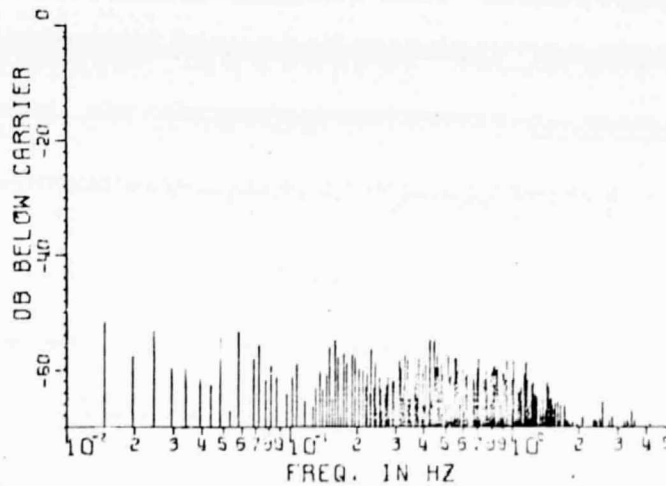20 GHZ RECEIVER
TAPE 110
TIME 142 17 10 13 905
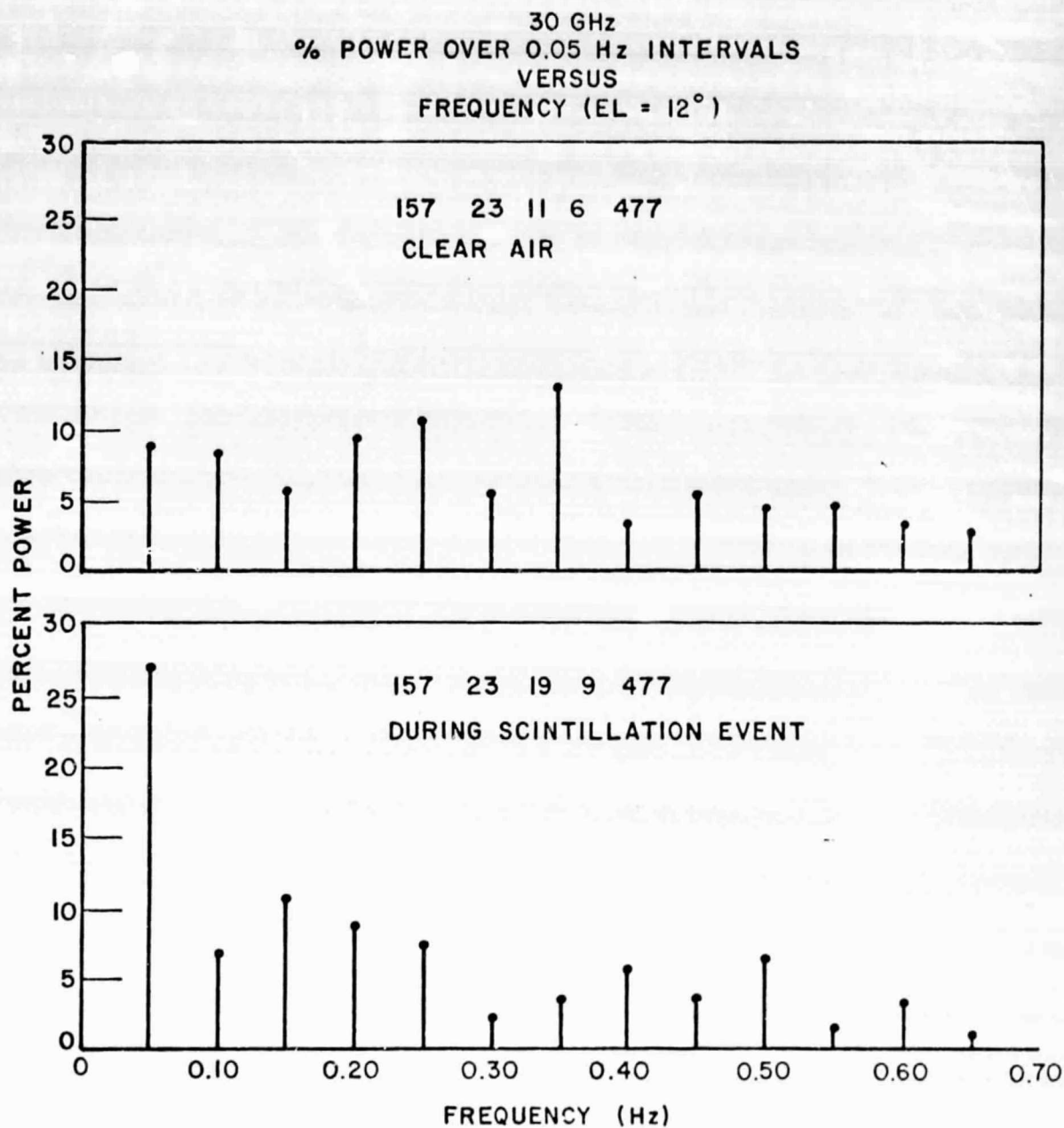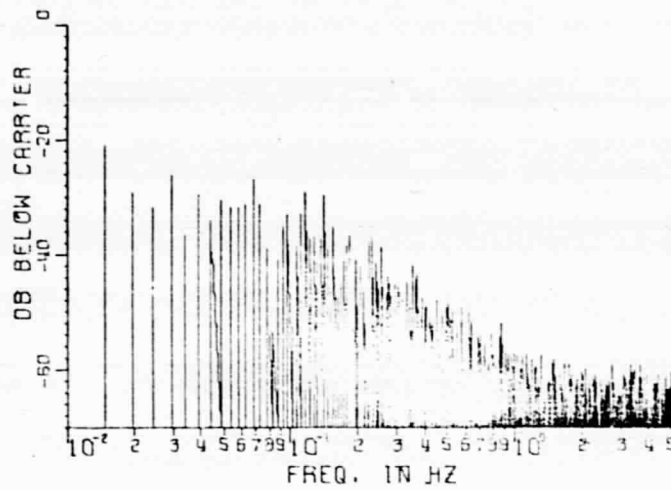

Fig. 17. Power spectrum at 42° elevation.

23

Fig. 18. Comparison of power spectra for clear air
case and scintillation event.

24

POWER SPECTRUM

30 GHZ RECEIVER

TAPE   111

TIME   163   16 17 45 307

POWER SPECTRUM   EL = 2°

20 GHZ RECEIVER

TAPE   111

TIME   163   16 17 45 307

Fig. 19. Power spectrum at 2° elevation.

25

Fig. 20. Cross-correlation between 20 and 30 GHz
signals at 12° elevation.

Fig. 21.   Cross-correlation between 20 and 30 GHz
signals at 2° elevation.

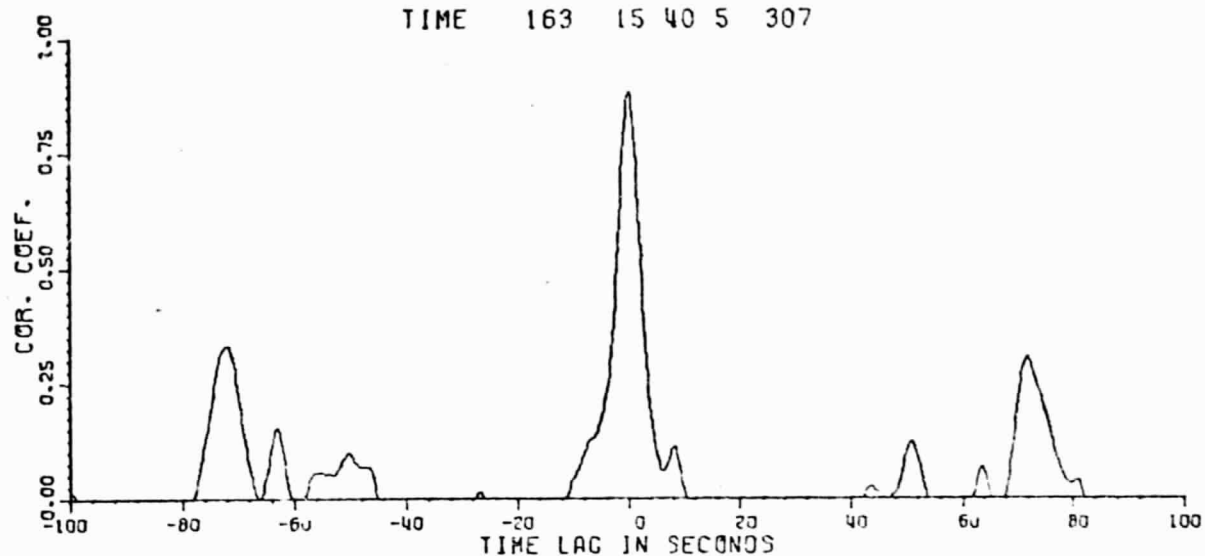One would expect low 20-30 GHz correlation if multipath were the dominant factor, because an arbitrary differential path length cannot produce simultaneous subtractive phasing at the two wavelengths employed. A simple exercise can readily demonstrate this point. Subtractive multipath phasing will occur at a wavelength of λ_1, if the difference between the two path lengths satisfies

$$\Delta L = (2n + 1) \frac{\lambda_1}{2} \quad , \quad n = 0,1,2,\cdots \quad . \tag{10}$$

Simultaneous subtractive phasing will occur at the second wavelength, λ_2, if

$$\Delta L = (2m + 1) \frac{\lambda_2}{2} \quad , \quad m = 0,1,2,\cdots \quad . \tag{11}$$

Therefore,

$$(2n + 1) \lambda_1 = (2m + 1) \lambda_2 \tag{12}$$

but, for this experiment

$$\lambda_1 = \frac{3}{2} \lambda_2 \tag{13}$$

so that

$$3/2 (2n + 1) = (2m + 1) \tag{14}$$

and, rearranging

$$6n = 4m - 1. \tag{15}$$

Noting that the left side of eq. (15) is even and the right side is odd, one may conclude that simultaneous subtractive phasing is impossible for the wavelengths employed. Hence, because the 20-30 GHz data are highly correlated, one may conclude that multipath is not the dominant scintillation mechanism.

All of the 20-30 GHz zero-lag correlation coefficients for elevation angles between $6°$ and $43°$, as well as their average, are plotted in Fig. 22. The experimental data for a frequency ratio
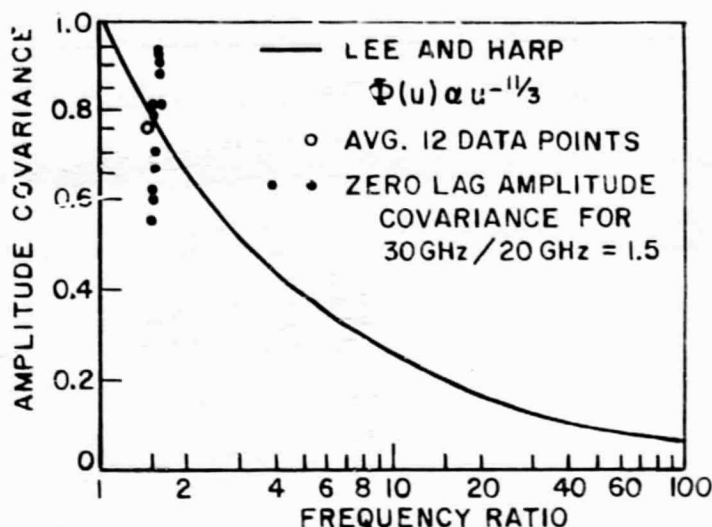
Fig. 22. Zero lag correlation coefficients for
elevation angles between 6° and 43°.
Theoretical curve from Lee and Harp,
Proc. IEEE, V. 57, p. 357, 1969.

30 GHz/20 GHz = 1.5 agrees quite well with the covariance calculated
by Lee and Harp using a Kolmogorov spectrum and tends to confirm
that a refractive mechanism is the dominant cause of amplitude
scintillations. This conclusion does not necessarily hold for
paths quite close to the horizon since multipath effects will
certainly become apparent as the beam approaches the horizon.

The cross-correlations between all 20-20, 30-30, and 20-30 GHz
pairs of propagation paths were also calculated for the two OSU
terminals located at a separation distance of 7 meters. The
correlation coefficients ranged from 0.1 to 0.8 for various
combinations. Single terminal 20-30 GHz pairs generally had
higher correlation coefficients than pairs with 7-meter spacing.
Although the data set for this type of measurement was limited, the
results tend to indicate that significant lack of correlation can
occur across the 7-meter separation distance.

CONCLUSION

The results of the OSU 20 and 30 GHz earth-satellite propagation measurements using the ATS-6 satellite have been presented. These results indicate that diversity gain is independent of frequency over the range 15 to 30 GHz and that diversity gain is relatively insensitive to baseline orientation for the 13 km separation distance employed. The diversity gain results agree well with the empirical relationship for diversity gain developed earlier.

Scintillations were found to be present at all times but increased in amplitude on occasion. The variance of these scintillations was found to be proportional to approximately the 11/6's power of the path length through the atmosphere. The peak-to-peak values of these scintillations varied from as low as 1 dB at high elevation angles to values in excess of 25 dB at an elevation angle of 2°. Most of the spectral power of these scintillations is located in the portion of the spectrum below a few Hertz; and, furthermore, the scintillations at 20 and 30 GHz were highly correlated. This behavior rules out the possibility of multipath as a dominant mechanism at elevation angles where the beam clears the horizon.

REFERENCES

NOTE: This reference list includes all reports, oral presentations, and publications generated to date under NASA Contract No. NAS5-21983.

1. D. B. Hodge, "ATS-F Millimeter Wavelength Propagation Experiment," Report 3863-1, July 1974.

2. D. B. Hodge and R. C. Taylor, Quarterly Report, "ATS-6 Millimeter Wavelength Propagation Experiment," Report 3863-2, September 1974.

3. D. B. Hodge and R. C. Taylor, Quarterly Report, "ATS-6 Millimeter Wavelength Propagation Experiment," Report 3863-3, March 1975.

4. D. M. Theobold and D. B. Hodge, Quarterly Report, "ATS-6 Milli-meter Wavelength Propagation Experiment, Report 3863-4, April 1975.

5. D. B. Hodge and D. M. Theobold, Quarterly Report, "ATS-6 Millimeter Wavelength Propagation Experiment," Report 3863-5, June 1975.

6. "Initial Results of OSU 20 and 30 GHz ATS-5 Propagation Measure-ments," D. B. Hodge and D. M. Theobold, 1975 URSI/USNC Meeting, Urbana, Illinois, June 1975.

7. "Scintillations Observed on the ATS-6 20 and 30 GHz Downlinks," D. B. Hodge and D. M. Theobold, URSI/USNC Meeting, Boulder, Colorado, October 1975.

8. "An Empirical Relationship for Path Diversity Gain," D. B. Hodge, accepted for publication, IEEE Trans. on Antennas and Propagation, March 1976.